



# Carbon dot-based artificial light-harvesting systems with sequential energy transfer and white light emission for photocatalysis

Chaoqun Ma<sup>a,1</sup>, Yuebo Wang<sup>a,1</sup>, Ning Han<sup>b,\*</sup>, Rongzhen Zhang<sup>a</sup>, Hui Liu<sup>a</sup>, Xiaofeng Sun<sup>a,\*</sup>, Lingbao Xing<sup>a,\*</sup>

<sup>a</sup>School of Chemistry and Chemical Engineering, Shandong University of Technology, Zibo 255000, China

<sup>b</sup>Department of Materials Engineering, KU Leuven, Leuven 3001, Belgium

## ARTICLE INFO

### Article history:

Received 14 April 2023

Revised 26 May 2023

Accepted 30 May 2023

Available online 2 June 2023

### Keywords:

Carbon dots

White light emission

Energy transfer

Antenna effect

Artificial light-harvesting system

Photocatalysis

## ABSTRACT

In this work, we designed and synthesized cationic carbon dots (CDs) with a size distribution of 1.6–3.7 nm, which exhibited dark blue fluorescence in the aqueous solution. Based on its excellent luminescence properties, we used it as an energy donor to construct a sequential artificial light-harvesting system (LHS) by employing the energy-matching dyes eosin Y disodium salt (EY) and sulforhodamine 101 (SR101), which could regulate the white light emission (Commission Internationale de l'Eclairage (CIE) coordinate: (0.30, 0.31)) with the energy transfer efficiency ( $\Phi_{ET}$ ) of 53.9% and 20.0%. Moreover, a single-step artificial LHS with white light emission (0.32, 0.28) can be constructed directly using CDs and dye solvent 43 (SR) with  $\Phi_{ET}$  and antenna effect (AE) of 48.8% and 6.5, respectively. More importantly, CDs-based artificial LHSs were firstly used in photocatalytic of  $\alpha$ -bromoacetophenone, with a yield of 90%. This work not only provides a new strategy for constructing CDs-based LHSs, but also opens up a new application for further applying the energy harvested in CDs-based LHSs to the field of the aqueous solution photocatalysis.

© 2024 Published by Elsevier B.V. on behalf of Chinese Chemical Society and Institute of Materia Medica, Chinese Academy of Medical Sciences.

Photosynthesis is the basis for all life activities, in which the sunlight is absorbed as light energy and then transformed into chemical energy in numerous chloroplast pigments through light-harvesting systems (LHSs) [1–7]. Inspired by this interesting process, many scientists are trying to construct artificial LHSs, which can effectively mimic natural photosynthesis [8–12]. The Förster resonance energy transfer (FRET) involves nonradiative dipole-dipole coupling, which provides an effective way to construct efficient artificial LHS. The process requires the distance between the energy donors and acceptors between 1 nm to 10 nm, and the energy is transferred from the donors to the acceptors under the excitation of the energy donors. Various artificial LHSs based on hydrogen bonding [13–15], host-guest interaction [16–21], coordination-induced self-assembly [22–25], supramolecular polymers [4,8], micelles or vesicles [9,26–30] and electrostatic interaction [29,30] have been constructed, which can efficiently transfer light energy. However, complex synthesis and separation processes are still unavoidable in the process of constructing these

LHSs. Therefore, it is urgent to develop new materials that can easy to synthesize and have excellent fluorescence properties to construct efficient artificial LHSs.

Carbon dots (CDs) [31–36] as a new luminescent material have been gradually introduced into the field of scientists benefitting from its advantages of good water solubility, high luminescence stability, easy syntheses, and low cost. At the same time, compared with traditional organic dyes, CDs overcome the shortcomings of organic dyes, such as luminescence instability, easy photobleaching, and easy-to-achieve surface functionalization, so CDs have a good application prospect in biochemical sensing, cell imaging, heavy metal detection, photocatalysis, drug carriers, photo-electronic devices and other fields [37–39]. However, the development and application of CDs as energy donors with excellent optical properties in light-harvesting systems are rarely reported. Since the fluorescence of CDs can be easily tuned, they can be used as good energy donors, and the wide emission band can ensure a high degree of coincidence with a variety of dye levels. In addition, there are a lot of functional groups around the CDs, endowing their good biocompatibility and adjustability. Recently, Zhou *et al.* reported a new srikaya-like artificial LHS based on electrostatic interaction by anionic graphene quantum dots (GQDs) as donors and porphyrin monomolecular micelles as acceptors [40]. Liu *et*

\* Corresponding authors.

E-mail addresses: ning.han@kuleuven.be (N. Han), xiaofengsun@sdut.edu.cn (X. Sun), lbxing@sdut.edu.cn (L. Xing).

<sup>1</sup> These authors contributed equally to this work.

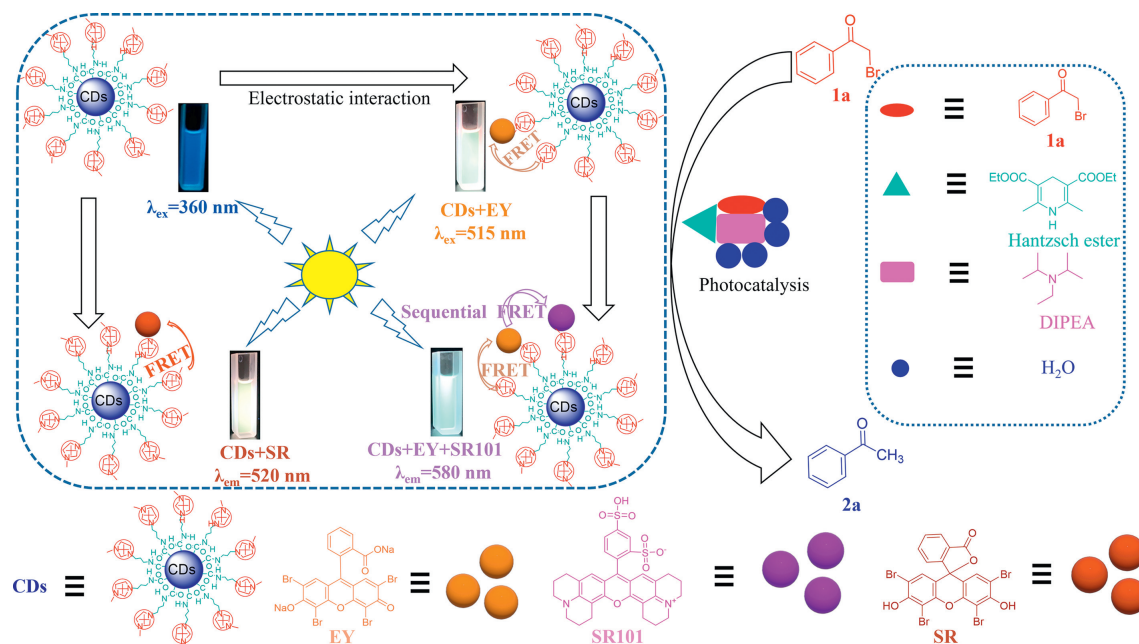


Fig. 1. Schematic diagram of artificial LHSs with efficient energy transfer process and white emission based on CDs.

al. used anionic CDs as energy donors and cationic supramolecular nanofibers formed by the complexation of styrylpyridinium-modified diarylethene and cucurbit[8]uril (CB[8]) as energy acceptors to form a broad spectra output ternary supramolecular combination and achieve pure white light emission in the process of luminous color conversion [41]. However, there are few studies on the construction of sequential energy transfer systems based on CDs and the application of using the harvested energy for photocatalysis.

Herein, we designed a novel strategy to introduce artificial LHSs containing CDs via a simple electrostatic interaction for photocatalysis dehalogenation of  $\alpha$ -bromoacetophenone in the aqueous solution (Fig. 1). After a series of tests including the zeta potential and steady-state spectra test, CDs were used as energy donors with energy level matching fluorescent dyes to construct three CDs-based artificial LHSs with the efficient energy transfer process and white emission. Then, the fluorescence lifetimes and fluorescence quantum yields of the three CDs-based artificial LHS were obtained respectively. Subsequently, to further use the energy harvested by the energy acceptors (eosin Y disodium salt (EY), sulforhodamine 101 (SR101), and solvent red 43 (SR)), we first applied the three CDs-based artificial LHSs for photocatalysis of  $\alpha$ -bromoacetophenone.

CDs were synthesized from citric acid and 1-aminopropyl-3-methylimidazolium bromine ([APMI][Br]) by hydrothermal method at 180 °C (Fig. S1 in Supporting information) and characterized by high-resolution transmission electron microscopy (HR-TEM) and X-ray diffraction (XRD). It can be seen from the results of HR-TEM that the as-prepared CDs are uniform in size and have a diameter of 1.6–3.7 nm (Fig. 2a). The XRD results of the CDs showed that there was a broadened peak near the diffraction angle of 24° ( $2\theta$ ), which revealed the amorphous nature of the CDs (Fig. 2b). CDs can be dissolved in an aqueous solution with dark blue fluorescence under UV light excitation. After the zeta potential test, the results showed that the positive potential of CDs was +13.7 mV (Fig. 2c). Then, we chose three normal fluorescent dyes EY, SR101, and SR, which showed negative potentials of –24.5 mV (Fig. 2d), –42.2 mV (Fig. 2e), and –26.9 mV (Fig. 2f), to construct LHSs with CDs through electrostatic interaction. Ultraviolet–visible (UV–vis) absorption and fluorescence emission spectra were em-

ployed to investigate the optical properties of CDs. A series of CDs aqueous solutions with different concentrations (10–100  $\mu\text{g}/\text{mL}$ ) were prepared for the UV–vis absorption test. It was found that the maximum absorption wavelength was 360 nm and the absorption increased gradually with the increasing of the concentrations, accompanying a slight red shift (Fig. 3a). At the same time, CDs with a concentration of 30  $\mu\text{g}/\text{mL}$  were selected for the fluorescence emission spectra test. The results showed that the emission band was 380–675 nm and the emission peak of CDs was centered at 455 nm (Fig. 3b), while the fluorescence quantum yield was 0.5%.

Because the CDs can exhibit excellent fluorescence properties in the aqueous solution, which was expected to be used as a good energy donor to construct CDs-based artificial LHSs. To construct artificial LHSs efficiently, the selection of fluorescence dyes in the FRET process with matching energy is very important. Therefore, EY and SR were selected as energy acceptors to fabricate artificial LHSs with CDs, because of the good overlap between the absorption band of EY or SR and the fluorescence band of CDs, in which the absorption band of EY was 450–550 nm (Fig. 3b) and the absorption band of SR was 425–550 nm (Fig. 3d). Moreover, the anionic energy acceptors EY and SR can interact with the positively charged energy donor CDs, in which the transfer distance between the donor CDs and the acceptors EY or SR became very closer to benefit for the energy transfer. The above two advantages provided an effective premise for the construction of CDs-based artificial LHS. When CDs were excited with a wavelength of 360 nm, the fluorescence emission at 455 nm decreased while the emission at 560 nm increased gradually with the addition of EY (acceptor) to the aqueous solution of CDs (donor). When 200  $\mu\text{L}$  EY (mass percent of CDs:EY at 14:1) was added into the aqueous solution of CDs, no more changes could be found in the fluorescence emission spectra, indicating the interaction between CDs and EY had reached equilibrium (Fig. 4a). The energy transfer efficiency ( $\Phi_{\text{ET}}$ ) and antenna effect (AE) of this system reached 53.9% (Fig. S2a in Supporting information) and 7.2 (Fig. S2b in Supporting information), while the fluorescence quantum yield was 1.5%.

More importantly, it can be observed in the CIE coordinate diagram that the color of the CDs+EY mixed solution changed from blue to blue-white (0.25, 0.31) (Fig. S3a in Supporting information),

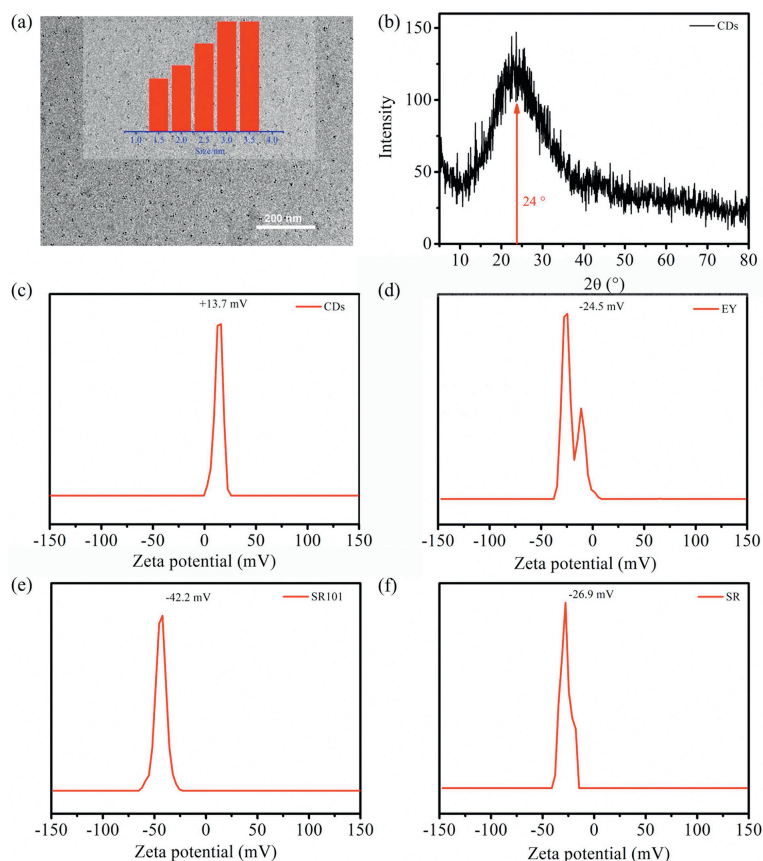


**Fig. 2.** (a) HR-TEM images of CDs; Inset: the particle size distribution diagram of CDs; (b) XRD images of CDs; zeta potentials of CDs (c), EY (d), SR101 (e), and SR (f) in the aqueous solution. [CDs] = 30  $\mu\text{g/mL}$ , [EY] =  $5.0 \times 10^{-5}$  mol/L, [SR101] =  $5.0 \times 10^{-5}$  mol/L, [SR] =  $1.0 \times 10^{-3}$  mol/L.

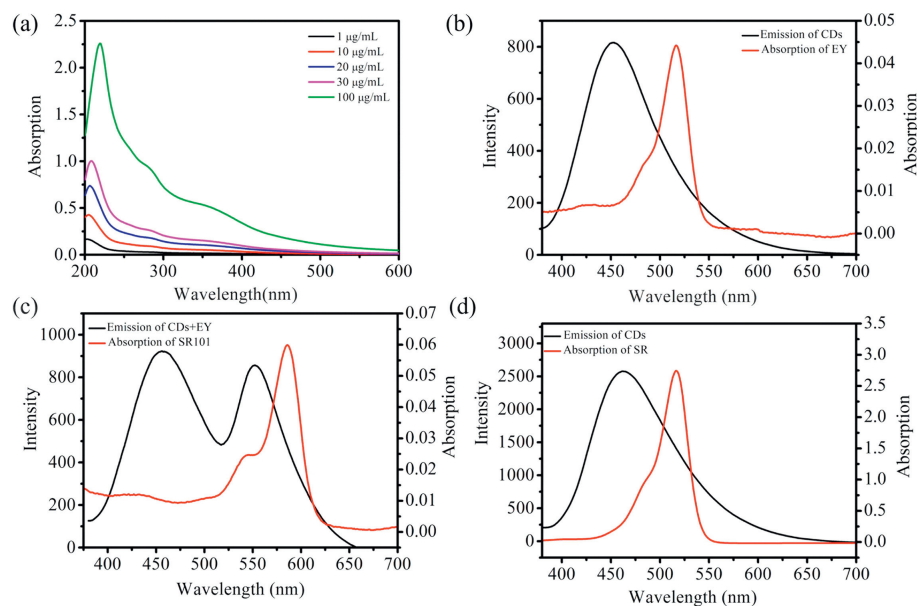


**Fig. 3.** (a) UV-vis absorption spectra of CDs aqueous solution with different concentrations (10–100  $\mu\text{g/mL}$ ). Fluorescence emission spectra of CDs ( $\lambda_{\text{ex}} = 360$  nm) and UV-vis absorption spectra of EY (b), SR101 (c), and SR (d). [CDs] = 30  $\mu\text{g/mL}$ , [EY] =  $5.0 \times 10^{-5}$  mol/L, [SR101] =  $5.0 \times 10^{-5}$  mol/L, [SR] =  $1.0 \times 10^{-3}$  mol/L.

indicating that there was an effective energy transfer between CDs and EY. In addition, we also titrated another acceptor SR using the same method. When 150  $\mu\text{L}$  SR (mass percent of CDs: EY at 1:1) was added into the aqueous solution of CDs, no more changes could be found in the fluorescence emission spectra, indicating the interaction between CDs and SR had reached equilibrium (Fig. 4b).

Meanwhile, the zeta potential of CDs+SR was +9.4 mV (Fig. S4 in Supporting information) compared to +13.7 mV of CDs, which further confirmed the binding of CDs and SR. The energy transfer efficiency ( $\Phi_{\text{ET}}$ ) and antenna effect (AE) of the system reached 48.8% (Fig. S2e in Supporting information) and 6.5 (Fig. S2f in Supporting information), while the fluorescence quantum yield was 4.5%.

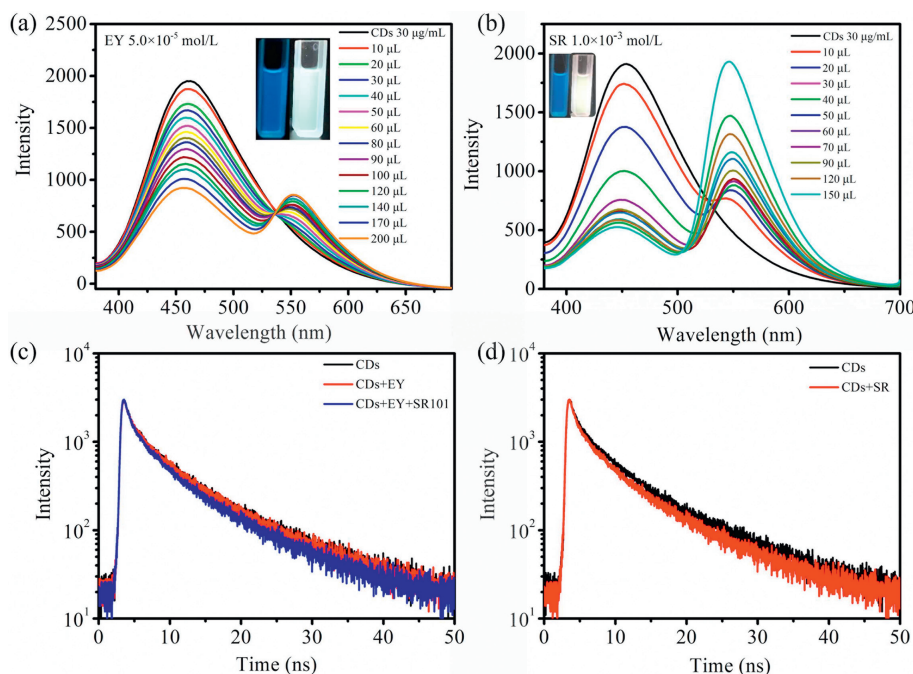


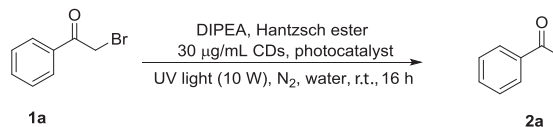
**Fig. 4.** (a) Fluorescence emission spectra of CDs with different amounts of EY in aqueous solution. Inset: Photos of CDs (left) and CDs+EY (right). (b) Fluorescence emission spectra of CDs with different amounts of SR in aqueous solution. Inset: Photographs of CDs (left) and CDs+SR (right). (c) Fluorescence decay profiles of CDs, CDs+EY, and CDs+EY+SR101. (d) Fluorescence decay profiles of CDs and CDs+SR. [CDs] = 30 µg/mL, [EY] =  $5.0 \times 10^{-5}$  mol/L, [SR101] =  $5.0 \times 10^{-5}$  mol/L, [SR] =  $1.0 \times 10^{-3}$  mol/L.

More importantly, it can be observed in the CIE coordinate diagram that the color of the CDs+SR mixed solution changed from blue to yellow-white (0.32, 0.28) (Fig. S3b in Supporting information), indicating that there was an effective energy transfer between CDs and SR. Subsequently, time-resolved fluorescence measurements showed that with the addition of the SR acceptors, the fluorescence time was significantly shortened from 0.7179 ns to 0.6795 ns, indicating that the corresponding energy transfer did occur between the donors and acceptors (Fig. 4d). Meanwhile, in order to verify the stability of the systems, fluorescence emission spectra were used to test CDs/dye composites (CDs+EY and CDs+SR) before and after one month of placement. The results showed that the fluorescence intensity did not change significantly, indicating that the constructed LHSs have good stability. At the same time, the mixed solutions (CDs+EY and CDs+SR) before and after one month was irradiated by the laser lamp, and it was found that the Tyndall effect was also found, which further proved that the CDs/dye complex had good stability (Fig. S5 in Supporting information).

Subsequently, to better simulate the process of photosynthesis, a negative potential dye SR101 containing a large energy level overlap with CDs+EY, whose absorption band appeared at 550–625 nm (Fig. 3c) was selected as the second energy acceptor. With the addition of SR101 into the CDs+EY mixed solution, the fluorescence intensity of CDs+EY (donor) at 560 nm decreased, while the emission of SR101 (the second acceptor) at 620 nm increased gradually. With the amounts of SR101 added into the CDs+EY mixed solution reaching 230 µL (mass percent of CDs+EY:SR101 at 10:1) (Fig. S6 in Supporting information),  $\Phi_{ET}$  and AE were calculated as 20.0% (Fig. S1c) and 2.1 (Fig. S1d), while the fluorescence quantum yield was 2.1%. At the same time, the fluorescent colors of the CDs+EY+SR101 mixed solution changed to red compared with the yellow-white of the CDs+EY mixed solution, which further proved the successful construction of an efficient two-step sequential artificial LHS based on CDs. It was worth mentioning that when 10 µL SR101 (mass percent of CDs+EY:SR101 at 230:1) was added into CDs+EY solution, the color of the mixed solution was bright white

**Table 1**

Photocatalytic dehalogenation of  $\alpha$ -bromoacetophenone under different conditions.<sup>a</sup>



Entry	Condition	Light irradiation	Yield <sup>b</sup> (%)
1	None	Yes	25
2	CDs	Yes	60
3	EY	Yes	55
4	SR	Yes	52
5	SR101	Yes	50
6	CDs+EY	Yes	90
7	CDs+EY+SR101	Yes	75
8	CDs+SR	Yes	85
9 <sup>c</sup>	CDs+EY	No	No reaction
10 <sup>c</sup>	CDs+EY+SR101	No	No reaction

<sup>a</sup> Reaction conditions: Bromoacetone (40 mg, 0.2 mmol), Hantzsch ester (56 mg, 0.22 mmol), *N,N*-diisopropylethylamine (DIPEA) (70 µL, 0.4 mmol), CDs+EY (30 µg/mL+200 µL) aqueous solution (5 mL), 10 W UV light, room temperature, nitrogen, 16 h.

<sup>b</sup> Isolated yields.

<sup>c</sup> Without a UV light.

and the CIE coordinate was (0.30, 0.31), which was very close to the white light point (0.33, 0.33) (Fig. S3a). Subsequently, time-resolved fluorescence measurements showed that with the addition of the EY and SR101 acceptors, the fluorescence time was significantly shortened from 0.7179 ns to 0.7045 ns, and 0.7045 ns to 0.6517 ns, which indicating that the corresponding energy transfer did occur between the donors and acceptors (Fig. 4c).

To make better use of the energy harvested from the energy acceptors (EY, SR, and SR101), we used three CDs-based artificial LHSs (CDs+EY, CDs+SR, and CDs+EY+SR101) for photocatalytic the dehalogenation of  $\alpha$ -bromoacetophenone. As shown in Table 1, in the presence of CDs+EY (mass percent of CDs:EY at 14:1), the yield reached 90% after irradiation with UV light for 16 h (Fig.

S7 in Supporting information). In contrast, under the same conditions, the yields of other systems including CDs, EY, SR, CDs+SR (mass percent of CDs:SR at 1:1), CDs+EY+SR101 (mass percent of CDs+EY:SR101 at 10:1), or without any catalyst were lower than that of CDs+EY. The good catalysis effect of the CDs+EY system may be due to the assembly of CDs and EY based on the electrostatic interaction, in which EY molecules were arranged in a more orderly manner and a higher energy transfer efficiency was obtained. Although the CDs+EY+SR101 system with a two-step sequential energy transfer process improved the light energy utilization efficiency, the second acceptor (SR101) harvested less energy than that of CDs+EY system and obtained a lower catalysis efficiency. The reason why the catalytic yield of CDs+SR was slightly lower than that of CDs+EY depended on the energy transfer efficiency.

After establishing optimal reaction conditions (mass percent of CDs:EY at 14:1), the photocatalytic dehalogenation of  $\alpha$ -bromoacetophenone derivatives was studied. As shown in Table S1 (Supporting information), for methyl  $\alpha$ -bromoacetophenone derivatives (**2b**), the system achieved a yield of 83%, while for methoxyl derivatives, the yields were 75% (**2c**), 94% (**2d**) and 95% (**2e**), respectively. High yields of **2f** (91%), **2g** (81%), and **2h** (80%) were also found for the following  $\alpha$ -bromoacetophenone derivatives with electron-withdrawing groups. In addition, we also studied 4-trifluoromethyl-2-bromoacetophenone and 2-bromoethyl naphthalene ketone to obtain 95% (**2i**) and 92% (**2j**) yields. These results indicated that CDs+EY had universal applicability as a catalyst for photocatalytic dehalogenation of  $\alpha$ -bromoacetophenone and its derivatives.

We have also proposed a mechanism of photocatalytic dehalogenation of  $\alpha$ -bromoacetophenone (**2a**). Firstly, the ground state CDs changed to the excited state of [CDs]\* under the UV light. Then, the state EY dye transferred [EY]\* after harvesting energy from [CDs]\*. The energy carried by the excited state EY\* oxidizes Hantzsch ester to EY<sup>-</sup>,  $\alpha$ -bromoacetophenone was reduced by EY<sup>-</sup> to the acetophenone radical, and EY<sup>-</sup> was reduced to EY. Eventually, the radical cation of Hantzsch ester is extracted by hydrogen atoms of the acetophenone radical and interacts with amine DIPEA to produce the by-product pyridine ester and the product acetophenone (**2a**) (Fig. S8 in Supporting information).

In conclusion, we have designed and synthesized a cationic CDs with dark blue luminescence, which can be used to construct artificial LHSs in an aqueous solution through electrostatic interaction with three anionic fluorescent dyes (EY, SR101, and SR). These three artificial LHSs can not only realize one-step efficient energy transfer from CDs to EY or SR, but also realize a sequential energy transfer system from CDs to EY and then to SR101. More importantly, we can also convert the light energy harvested by the artificial LHSs into chemical energy and realize the application of photocatalytic dehalogenation reaction, and exhibit good universality and high-efficiency photocatalytic activity. This work innovatively applied CDs for the construction of artificial LHSs and provided a new idea for the application of CDs in the field of photocatalysis.

### Declaration of competing interest

The authors declare that they have no known competing financial interests or personal relationships that could have appeared to influence the work reported in this paper.

### Acknowledgments

We are grateful for the financial support from the National Natural Science Foundation of China (Nos. 52205210 and 22002075) and the Natural Science Foundation of Shandong Province (Nos. ZR2020MB018 and ZR2022QE033).

### Supplementary materials

Supplementary material associated with this article can be found, in the online version, at doi:10.1016/j.ccl.2023.108632.

### References

- [1] H.Q. Peng, L.Y. Niu, Y.Z. Chen, et al., *Chem. Rev.* 115 (2015) 7502–7542.
- [2] K. Wang, K. Velmurugan, B. Li, et al., *Chem. Commun.* 57 (2021) 13641–13654.
- [3] Y.X. Hu, W.J. Li, P.P. Jia, et al., *Adv. Opt. Mater.* 8 (2020) 2000265.
- [4] C.B. Winiger, S. Li, G.R. Kumar, et al., *Angew. Chem. Int. Ed.* 53 (2014) 13609–13613.
- [5] C.L. Sun, H.Q. Peng, L.Y. Niu, et al., *Chem. Commun.* 54 (2018) 1117–1120.
- [6] G.R. Fleming, G.S. Schlau-Cohen, K. Amarnath, et al., *Faraday Discuss.* 155 (2012) 27–41.
- [7] H. Kashida, H. Azuma, R. Maruyama, et al., *Angew. Chem. Int. Ed.* 59 (2020) 11360–11363.
- [8] D. Zhang, Y. Liu, Y. Fan, et al., *Adv. Funct. Mater.* 26 (2016) 7652–7661.
- [9] J. Huang, Y. Yu, L. Wang, et al., *ACS Appl. Mater. Interfaces* 9 (2017) 29030–29037.
- [10] B. Kriete, A.S. Bondarenko, R. Alessandri, et al., *J. Am. Chem. Soc.* 142 (2020) 18073–18085.
- [11] X. Fan, C.P. Teng, J.C.C. Yeo, et al., *Macromol. Rapid Commun.* 42 (2021) 2000716.
- [12] T. Huang, Z. Zhu, R. Xue, et al., *Langmuir* 34 (2018) 5935–5942.
- [13] H.Q. Peng, C.L. Sun, L.Y. Niu, et al., *Adv. Funct. Mater.* 26 (2016) 5483–5489.
- [14] T. Xiao, H. Wu, G. Sun, et al., *Chem. Commun.* 56 (2020) 12021–12024.
- [15] H.Q. Peng, J.F. Xu, Y.Z. Chen, et al., *Chem. Commun.* 50 (2014) 1334–1337.
- [16] J.J. Li, Y. Chen, J. Yu, et al., *Adv. Mater.* 29 (2017) 1701905.
- [17] Z. Xu, S. Peng, Y.Y. Wang, et al., *Adv. Mater.* 28 (2016) 7666–7671.
- [18] H.J. Kim, D.R. Whang, J. Gierschner, et al., *Angew. Chem. Int. Ed.* 55 (2016) 15915–15919.
- [19] X.M. Chen, Q. Cao, H.K. Bisoyi, et al., *Angew. Chem. Int. Ed.* 59 (2020) 10493–10497.
- [20] X.H. Wang, N. Song, W. Hou, et al., *Adv. Mater.* 19 (2013) 1903962.
- [21] X. Li, S. Yu, Z. Shen, et al., *J. Colloid. Interface Sci.* 617 (2022) 118–128.
- [22] C.B. Huang, L. Xu, J.L. Zhu, et al., *J. Am. Chem. Soc.* 139 (2017) 9459–9462.
- [23] K. Acharyya, S. Bhattacharyya, H. Sepehrpour, et al., *J. Am. Chem. Soc.* 141 (2019) 14565–14566.
- [24] Z. Zhang, Z. Zhao, Y. Hou, et al., *Angew. Chem. Int. Ed.* 58 (2019) 8862–8866.
- [25] P. Wang, X. Miao, Y. Meng, et al., *ACS Appl. Mater. Interfaces* 20 (2021) 22630–22639.
- [26] H.Q. Peng, Y.Z. Chen, Y. Zhao, et al., *Angew. Chem. Int. Ed.* 51 (2012) 2088–2092.
- [27] Y. Liu, J. Jin, H. Deng, et al., *Angew. Chem. Int. Ed.* 55 (2016) 7952–7957.
- [28] Y. Zhao, *Langmuir* 32 (2016) 5703–5713.
- [29] C.Q. Ma, X.L. Li, N. Han, et al., *J. Mater. Chem. A* 10 (2022) 16390–16395.
- [30] C.Q. Ma, N. Han, R.Z. Zhang, et al., *J. Colloid. Interface Sci.* 634 (2022) 54–62.
- [31] S.N. Baker, G.A. Baker, *Angew. Chem. Int. Ed.* 49 (2010) 6726–6744.
- [32] S. Zhang, Y. Yang, Y. Zhai, et al., *Chin. Chem. Lett.* 34 (2023) 107652.
- [33] Z. Wei, B. Wang, M. Xie, et al., *Chin. Chem. Lett.* 33 (2022) 751–756.
- [34] X. Yang, X. Li, B. Wang, et al., *Chin. Chem. Lett.* 33 (2022) 613–625.
- [35] S. Chandra, P. Das, S. Bag, *Nanoscale* 3 (2011) 1533–1540.
- [36] A. Salinas-Castillo, M. Ariza-Avidad, C. Pritz, *Chem. Commun.* 49 (2013) 1103–1105.
- [37] S.Y. Lim, Shen, Z. Gao, *Chem. Soc. Rev.* 44 (2015) 362–381.
- [38] H. Yu, R. Shi, Y. Zhao, *Adv. Mater.* 28 (2016) 9454–9477.
- [39] X. Sun, K. Yin, B. Liu, et al., *J. Mater. Chem. C* 5 (2017) 4951–4958.
- [40] Y. Liu, S. Li, K. Li, et al., *Chem. Commun.* 60 (2016) 9394–9397.
- [41] H. Wu, Y. Chen, X. Dai, et al., *J. Am. Chem. Soc.* 16 (2019) 6583–6591.